Atmospheric HCFC-22, HFC-125, and HFC-152a at Cape Point, South Africa

HCFCs and HFCs in the atmosphere at Cape Point, South Africa

Brett Kuyper[1], Daniel Say[2], Casper Labuschagne[3], Timothy Lesch[1], Warren R. Joubert[3], Damien Martin[2], Dickon Young[2], M. Anwar H. Khan[2], Matthew Rigby[2], Anita L. Ganesan[4], Mark F. Lunt[5], Alistair J. Manning[2,6], Simon O'Doherty[2], Michael T. Davies-Coleman[1], Dudley E. Shallcross[1,2]

[1]Department of Chemistry, University of the Western Cape, Bellville 7535, South Africa

[2]Atmospheric Chemistry Research Group, School of Chemistry, University of Bristol, Bristol, BS8 1TS, United Kingdom

[3]Climate and Environmental Research and Monitoring, South African Weather Service, Stellenbosch 7600, South Africa

[4]School of Geographical Sciences, University of Bristol, Bristol, BS8 1SS, United Kingdom

[5]School of Geosciences, University of Edinburgh, Edinburgh, EH9 3JW, United Kingdom

[6]Hadley Centre, The Met Office, Exeter, EX1 3PB, United Kingdom

ABSTRACT

One hydrochlorofluorocarbon and two hydrofluorocarbons (HCFC-22, HFC-125, HFC-152a) were measured in air samples at the Cape Point observatory (CPT), South Africa during 2017. These data represent the first such atmospheric measurements of these compounds from south western South Africa. Our results indicate Cape Town to be the dominant source of the halocarbon pollution events observed at CPT. Baseline atmospheric growth rates were estimated to be 8.36 ppt yr^{-1}, 4.10 ppt yr^{-1} and 0.71 ppt yr^{-1} for HCFC-22, HFC-125 and HFC-152a, respectively. The CPT measurements were combined with an inverse model to investigate the possibility of estimating emissions for South Africa. The results exhibited some dependency on the choice of prior – this could be reduced with further measurements, particularly in the winter months during which the instrument was down, but which coincided with a maximum in the sensitivity of CPT to terrestrial sources. At 3.6 (1.3 – 8.7) Gg yr^{-1} for HCFC-22, 1.6 (0.8 – 2.6) Gg yr^{-1} for HFC-125, and 0.13 (0.10 – 0.19) Gg yr^{-1} for HFC-152a, the current contribution of South Africa to the global emissions of these gases is relatively minor. Further measurements could provide a useful means to verify progress made by South Africa towards its Montreal Protocol commitments.

Keywords: HFC, HCFC, South Africa, climate, greenhouse gases, ozone depleting substances, emissions

INTRODUCTION

The phasing-out of the industrial production of chlorofluorocarbons (CFCs), as a direct consequence of the Montreal Protocol, has led to an increase in the production and use of hydrochlorofluorocarbons (HCFCs) and hydrofluorocarbons (HFCs) as substitutes. Commonly used as refrigerants in air conditioners and in the production of insulating foams. HCFCs and

HFCs also find widespread applications as solvents used in lubricants, coatings and cleaning fluids. The presence of a reactive hydrogen atom in the molecular structures of HCFCs and HFCs results in these compounds being more susceptible to attack and degradation in the troposphere through reaction with hydroxyl radicals (OH).[1,2] HFCs have zero Ozone Depletion Potentials (ODP) as they contain no chlorine or bromine atoms and, despite the presence of chlorine in HCFCs these compounds have lower ODPs than the CFCs they replace.[3] Conversely, HCFCs and HFCs both have an immediate and significant effect on the Earth's climate due to their high global warming potentials (GWP).[4,5] Given their non-negligible ODPs and high GWPs,[6] the industrial production of HCFCs has been controlled under the Montreal Protocol and its amendments since 1992, and owing to their high GWPs, the production of HFCs will now be regulated following the Kigali amendment to the Protocol.[7,8]

HCFC-22 ($CHClF_2$), which has a tropospheric lifetime of 11.9 years[9], was introduced in the early 1990s as a replacement for CFCs and is the most abundant HCFC in the atmosphere[10]. The GWP of HCFC-22 is 1760 integrated over a 100-yr time horizon (GWP_{100})[9] and its ODP is 0.055.[11] The principal removal process for this compound from the atmosphere is reaction with OH ($k_{OH} = 5.0 \times 10^{-15}$ cm^3 $molecule^{-1}$ s^{-1} at 298 K).[12] Following a maximum global mean growth rate in 2007 of 8.2 ppt yr^{-1}, the rate of growth had decreased by 2015 to 3.7 ppt yr^{-1} (-54%).[11] The emissions of HCFC-22 have now stabilized at approximately 370 Gg yr^{-1} (2016) due to the freezing of HCFC production and consumption for dispersive (emitted to the atmosphere) uses in developing countries.[9,13] Production is limited to existing chemical plants and no increase in production is permitted under the Montreal Protocol guidelines. Currently, the main source of emission of HCFC-22 into the atmosphere is a result of leakage from refrigeration equipment either during use, servicing or final disposal, rather than from the chemical plants in which it is

produced.[14] Traditionally, emissions from leakage and servicing were thought to be relatively constant throughout the year.[15] However, more recent studies have suggested that there is significant seasonality in the emission rates of HCFC-22. Xiang et al.[16] estimated that emissions of HCFC-22 were over twice as large during summer months, compared to the winter. While this seasonal cycle is observed globally, the magnitude is larger in the northern hemisphere.[16] The authors proposed that the increased usage rates and ambient temperatures (resulting in greater charge pressures and hence greater leakage) generally associated with summer months as potential reasons for the observed seasonality.

HFC-125 (CF_3CHF_2) is the third most abundant HFC and currently makes the third largest contribution of the HFCs to atmospheric radiative forcing value with a GWP_{100} of 3500.[9,17,18] The atmospheric lifetime of HFC-125 is estimated to be 31 years[9] and this trace gas is removed from the atmosphere by reaction with OH resulting in *inter alia* carbonyl fluoride and trifluoromethanol degradation products. In 2015, the global average mixing ratio of HFC-125 was 18.4 ppt in the lower troposphere with an estimated growth of 2.3% per annum for the period of 1995-2015.[11] HFC-125 is almost exclusively used in blends with HFC-134a, HFC-143a and HFC-32. Common examples of these blends include R-410A (50% by wt. HFC-125, 50% by wt. HFC-32) and R-407C (52% by wt. HFC-134a, 25% by wt. HFC-125, 23% by wt. HFC-32). Both blends were designed as replacements for HCFC-22, in applications including domestic air-conditioning and commercial refrigeration. Commercial refrigeration systems, in particular, are notorious for their high leakage rates, with as much as 30% charge loss per year.[19] The rapid increase in global HFC-125 mixing ratios is well documented (e.g. Lunt et al.[20]; Li et al.[21]).

HFC-152a (CH_3CHF_2) has a relatively small GWP of 138[17] and a significantly shorter atmospheric lifetime of approximately 1.5 years[9,22], compared with other HFCs. Consequently,

HFC-152a is often used as a replacement for CFCs, various HCFCs and HFC-134a in technical aerosol applications, foam blowing and mobile air-conditioners. A rapid accumulation of HFC-152a in the atmosphere up to 2012, with increases of 8.9 ppt (1992 – 2012) and 3.7 ppt (1998 – 2012) for the Northern and Southern Hemispheres respectively, were reported.[22] However, the global mean mixing ratio has since stabilized, with a global mean growth rate post-2012 that does not differ significantly from 0 ppt yr^{-1} (-0.06 ± 0.05 ppt yr^{-1})[22]. Global emissions were estimated to be 52.5 ± 20.1 Gg yr^{-1} in 2014.[22]

The production and consumption of HCFCs is controlled by amendments to the Montreal Protocol. Specifically, the HCFC Phase-out Management Plan (HPMP) seeks to define targets for the reduction of HCFC consumption in developing countries such as South Africa. Under stage two of the HPMP, these countries agreed to freeze their consumption of HCFCs by 2013, followed by a 10% reduction by 2016. A complete ban on the production and consumption of HCFCs for dispersive applications is planned for 2030.[23] South Africa is expected to ratify the Kigali Amendment to the Montreal Protocol, which sets out phase-down targets for HFCs. However, developing countries will not be required to make their first reductions until 2040.

Given the greater population and industrialization in the Northern Hemisphere, a North-South interhemispheric gradient has been established for all of these compounds.[11,22] The number of *in-situ* measurements of HCFCs and HFCs available from Northern Hemispheric sites exceeds those available from the Southern Hemisphere. Continuous measurements of three CFCs (CFC-11, CFC-12 and CFC-113) and TCE have been made at the Cape Point Global Atmospheric Watch Station, South Africa over the period 1979-2015.[24] Extension of the range of tropospheric HCFC and HFC concentrations measured at sites in the Southern Hemisphere is required for more robust constraints on global, southern-hemispheric and regional emissions estimates. In this

study, we report the 2017 time series of atmospheric mixing ratios of HCFC-22, HFC-125 and HFC-152a at Cape Point, South Africa. We consider variations in the mixing ratios of each gas with respect to various meteorological parameters (e.g. wind speed and direction) and use an inverse model to provide the first documented top down emissions estimates of HCFC-22, HFC-125 and HFC-152a for South Africa.

METHODS

Global Atmospheric Watch Monitoring station

The South African Weather Service manage and maintain the Global Atmospheric Watch (GAW) monitoring station at Cape Point (34.5º S, 18.2º E) situated approximately 60 km south of the City of Cape Town (population ~4 million). The station is situated on an elevated peninsula (230 m above sea level) extending out into the south Atlantic (Figure 1). The local seasonal synoptic patterns around Cape Town results in predominantly clean marine air arriving at Cape Point during austral summer and occasionally anthropogenically modified air arriving during austral winter.[24,25] The differing air mass sources are driven by South Atlantic High Pressure (SAHP) system which occupies a latitudinal position roughly in line with Cape Town during summer, driving strong south-easterly winds, drawing air from deep in the south Atlantic, towards Cape Point.[25–27] The SAHP system retreats to the north during austral winter, thus allowing transient low-pressure systems to impact Cape Town and Cape Point.[25–28]

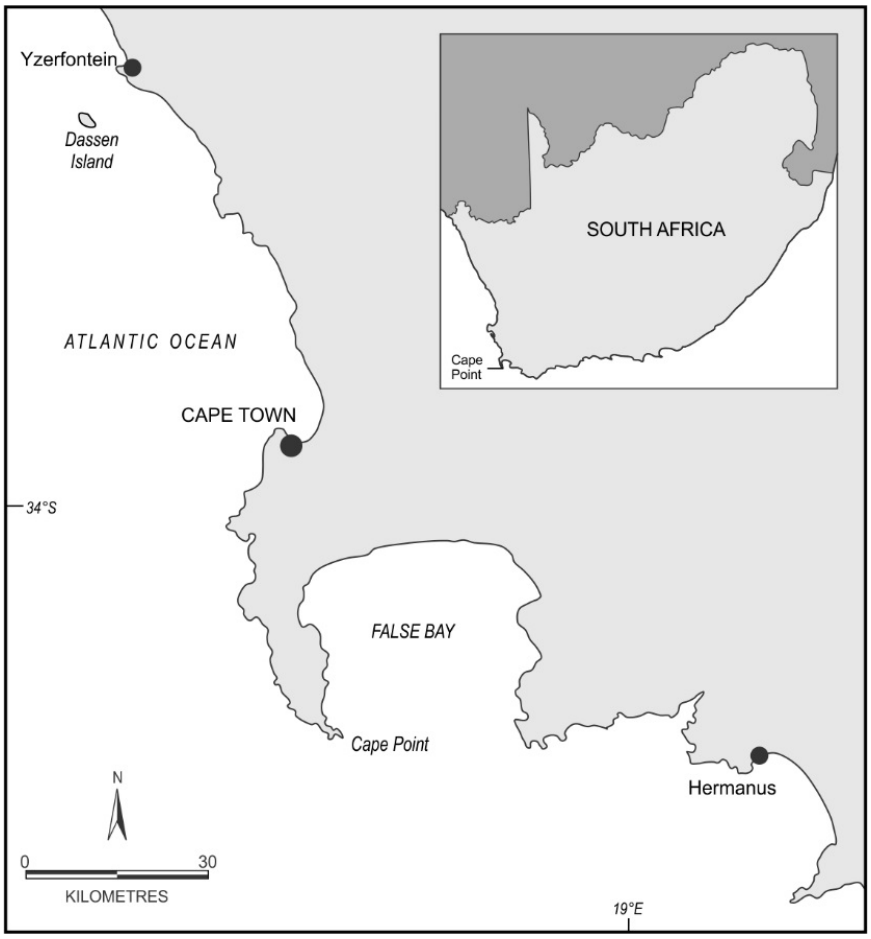

Figure 1. Cape Point and the GAW monitoring station in relation to Cape Town and the south Atlantic Ocean.

Cape Point Gas Chromatograph-Mass Spectrometer

An Agilent gas chromatograph-mass spectrometer (GC-MS, 6890/5973N) with a custom-built adsorption/desorption system (ADS) was used to measure HCFC and HFC mixing ratios in the atmosphere at Cape Point.[29] Air samples for analysis were drawn through a 15 m x ¼" OD stainless steel sampling from above the laboratory at ~17 l min^{-1} by a diaphragm pump (GAST, Miniature Diaphragm Pump 22D). Samples and standards were autonomously pre-concentrated

on a triple bed microtrap (3 mg Carbotrap B; 5 mg Carboxen 1003; 4 mg Carboxen 1000) at -50 ºC in the ADS.[30,31] Following pre-concentration on the microtrap, samples or standards were heated to 240 ºC and injected directly on to the column (CP Sil-5, 100m x 0.32 mm x 5 µm) at 240 ºC. Separation of the injected sample was achieved with a helium carrier flow (1.8 ml min^{-1}) and temperature programme with an initial isothermal period (30 ºC, 12 min) and temperature gradient (10 ºC min^{-1} to 150 ºC).

A short-term working standard, filled at Cape Point under baseline conditions, was analysed alternately to each air sample, to account for instrument drift. Calibrated mixing ratios were assigned to short-term working standards from an external long-term working standard tank which was calibrated using the Advanced Global Atmospheric Gases Experiment (AGAGE) Medusa GC-MS at Mace Head.[32,33] The procedure provided a direct comparison of the short-term working standard with the relevant Scripps Institute of Oceanography (SIO) primary calibration scales.[32] The calibration of the long-term working standard (filled at Mace Head) had mixing ratio values assigned from SIO-05 (HCFC-22 and HFC-152a) and SIO-14 (HFC-125). A complete description of the ADS-GC-MS system and set up can be found in Simmonds et al.[29]

Baseline classification algorithm

A statistical method based on the Advanced Global Atmospheric Gases Experiment (AGAGE) pollution algorithm was developed to identify baseline samples within long-lived trace gas mole fraction datasets. A full description can be found in the SI and the appendix to O'Doherty et al.[34] and Simmonds et al.[22]. In brief, a second order polynomial is fitted to the daily minima over a 121-day window. The polynomial was subtracted from each data point in the window, creating a

matrix of distances. Measurements that were larger than 3 times the median of the distances were marked as 'polluted'. This was repeated all the 'polluted' marked data removed. Measurements between 2-3 times the median were marked as 'possibly polluted'. In the final step 'possibly polluted' measurements were tested for adjacency with 'polluted' measurements.

Atmospheric dispersion modelling using NAME

The U.K. Meteorological (Met.) Office's Lagrangian atmospheric dispersion model, NAME (Numerical Atmospheric dispersion Modelling Environment), was used to simulate 30-day back-trajectories for each atmospheric measurement.[35] The NAME model was driven by meteorological fields derived from the operational analysis of the U.K. Met. Office Numerical Weather Prediction model, the Unified Model (UM), at an approximate horizontal resolution of 17 km in 2017 (reduced to ~12 km from 11th July 2017). The model domain spanned from 64° S to 4.3° N, and from 50° W to 87.3° E, covering southern Africa and the south Atlantic (Figure 2). Particles were released into the model domain from randomly generated points on a 20 m vertical line, centred on the Cape Point inlet (30 m above ground level) at a rate of 333 particles min^{-1}. All particles were assumed to be inert throughout the length of each 30-day simulation. Given the long lifetimes of the HCFC and HFCs studied here, this assumption can be made with very little loss of accuracy. At the edges of the NAME model domain, the 3-dimensional location and time at which each particle left the domain was recorded to provide sensitivity to mole fraction boundary conditions.

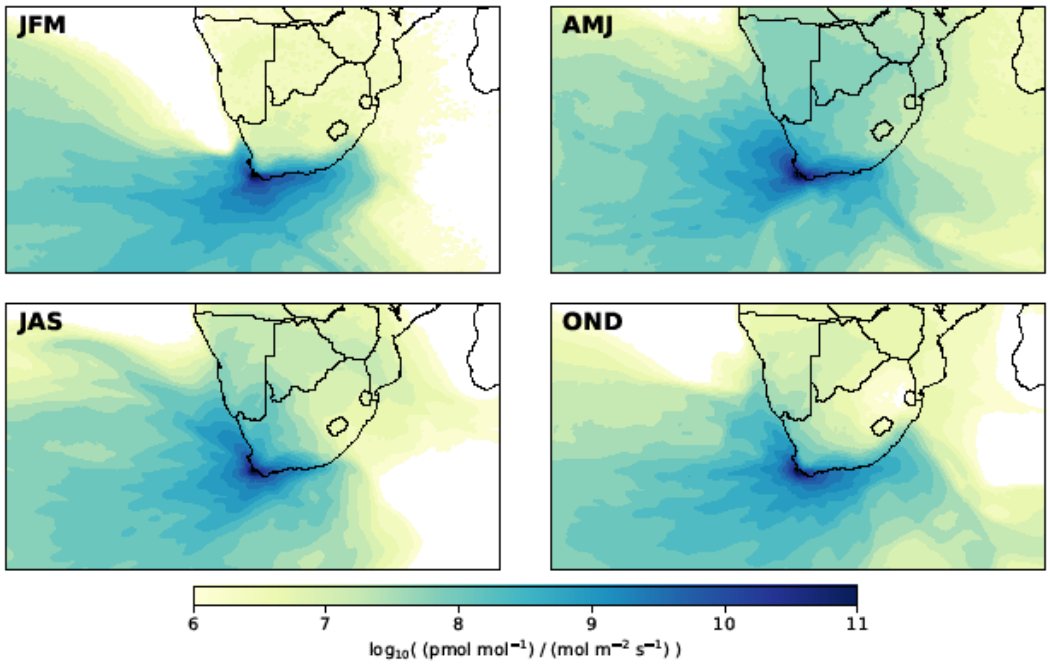

185

186**Figure 2: Mean 2017 quarterly air history footprints at Cape Point using the NAME model.**

187

188Estimating emissions using a hierarchical trans-dimensional Bayesian 189framework

190 A hierarchical trans-dimensional Bayesian framework was used to estimate South Africa's 191halocarbon emissions using the atmospheric measurements made at Cape Point. A full 192description of the inverse method can be found in Lunt et al.[36] The hierarchical treatment of 193uncertainties is described by Ganesan et al.[37] This inverse method has been used to estimate 194halocarbon emissions from other regions.[38,39] In short, the inverse approach attempts to solve for 195a parameters vector, $\boldsymbol{x}$ (including the flux grid and boundary conditions), using a set of 196atmospheric observations, $\boldsymbol{y}$. The system starts from an *a priori* flux field, $\boldsymbol{x}_{ap}$, which is adjusted 197using the atmospheric measurements in order to estimate the posterior flux field, $\boldsymbol{x}$, in

conjunction with a linear model, **H**. **H** is a Jacobian matrix of sensitivities which describes the relationship between changes in atmospheric mixing ratio and the parameters vector, $\boldsymbol{x}$. In a traditional Bayesian set-up, uncertainty in the *a priori* emissions ($\boldsymbol{x}_{ap}$) and model-measurement mismatch ($\boldsymbol{\varepsilon}$) are defined prior to the inversion. Hence, they are based on a subjective decision by the investigator. However, the choice of uncertainties has been shown to significantly influence the posterior solution. The hierarchical framework attempts to reduce the influence of this subjectivity by introducing hyper-parameters which define the uncertainties within these uncertainties.

A reversible-jump Markov Chain Monte Carlo algorithm (rj-MCMC) was used to estimate the posterior solution.[36] For each species, the rj-MCMC algorithm was run for a chain length of 400,000. The first 100,000 iterations were discarded to ensure that the system had no knowledge of the initial state. The remaining 400,000 iterations were then thinned via sub-sampling of every 100th iteration, resulting in 4000 samples, which were used to form the posterior PDFs. The emission estimates discussed in the following sections represent the means of these PDFs, with the corresponding uncertainty estimated by the 95th percentile confidence interval of the same PDFs.

A priori emissions

Little detailed information is available for South Africa's halocarbon emissions. Therefore, *a priori* emissions were constructed from a variety of sources which together represent the existing state of knowledge. In the absence of emissions data, HCFC-22 a priori emissions were estimated using consumption data from South Africa's most recent HPMP report, which was

estimated at 3.16 Gg yr^{-1} in 2009. In general, consumption is not a good approximation for emissions magnitudes (as, for this gas, emissions are likely dominated by release from the bank). However, as no estimates exist for South African emissions, we use consumption statistics as a proxy for emissions, but with a very large uncertainty (see below), on the assumption that they are of a similar order of magnitude to emissions. For HFC-125 and HFC-152a, emissions were taken from the EDGAR v4.2 emissions inventory, which reports gridded emissions data up to 2009. For all three gases, the a priori emissions total was distributed across the inverse model domain using the National Oceanic and Atmospheric Administration (NOAA) DMSP-OLS (Defence Meteorological Program - Operational Line-Scan System) satellite night-light data. These data are available at the increment of 30 arc second from https://ngdc.noaa.gov/eog/data/web_data/v4composites/. Night-lights have been shown to correlate with population density,[40] and hence this distribution is expected to be roughly representative of the sources of all three domestically consumed halocarbons. In each instance, the *a priori* emissions were given a 100% uncertainty, with the magnitude of this uncertainty further described by a uniform PDF with upper and lower bounds of 50% and 400% respectively. This PDF was explored within the inversion.

Boundary conditions

We incorporate boundary conditions to account for emissions from outside of the model domain. Uniform mixing ratio 'curtains' were estimated using output from the AGAGE 12-box model; an extension of the work by Rigby et al.[41] The 12-box model resolves baseline mixing ratios for four semi-hemispheres. For each month in which measurements were obtained, the simulated mixing ratio from latitude bands 0-30° N, 0-30° S and 30-90° S were assigned to the

North, East and West and South boundaries of the model domain respectively. The sensitivity of each measurement to the boundary conditions was estimated by mapping the exit locations of particles from the model domain for each measurement. The *a priori* boundary conditions were adjusted within the inversion.

RESULTS AND DISCUSSION

Cape Point measurements and observations

The baseline mixing ratios of one hydrochlorofluorocarbon and two hydrofluorocarbons (HCFC-22, HFC-125, HFC-152a) were determined from measurements made at the Cape Point Global Atmospheric Watch Station in 2017. The measurements were clustered along a baseline for the three species with occasional elevated data points (Figure 3). The mean mixing ratios observed at Cape Point were: HCFC-22: 237.80 ± 12.31 ppt; HFC-125: 22.47 ± 1.78 ppt and HFC-152a: 6.44 ± 5.32 ppt. The Cape Point HCFC-22 and HFC-125 mixing ratios increased throughout the year, in contrast with HFC-152a which displayed a small seasonal cycle. The increase through the year for HCFC-22 and HFC-125 was particularly noticeable for the last three months of 2017. Variability within the HCFC-22 and HFC-125 mixing ratios, particularly in the early part of the year, were observed. Changes in wind direction, and therefore source contributions, likely contributed significantly to the observed variability.

The HFC-152a mixing ratio increased between February and May, which continued in June. Following the winter maximum, the HFC-152a mixing ratios decreased through the latter half of the year. A lower rate of growth in the HFC-152a mixing ratios, compared with HCFC-22 and HFC-125, was observed over the year. The HFC-152a mixing ratios displayed a maximum in

austral winter and minima in January and December. The seasonal cycle observed in the HFC-152a mixing ratios was likely driven by the winter minimum OH concentration. The shorter atmospheric life of HFC-152a compared with HCFC-22 and HFC-125 highlights the sensitivity of this compound to reaction with OH, resulting in the observed seasonal cycle.

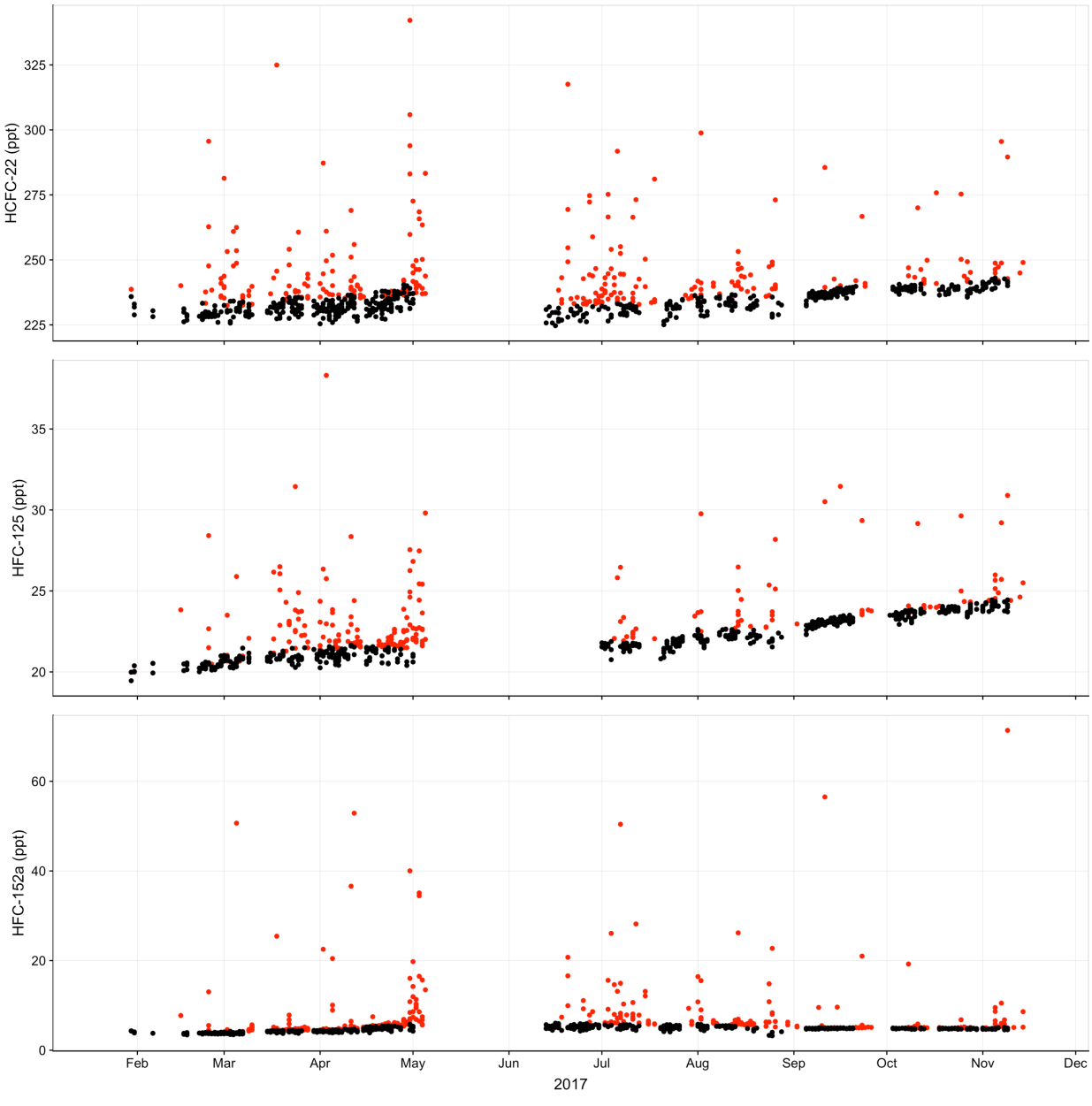

Figure 3. Time series of the HCFC and HFCs measured in the atmosphere at Cape Point. The gaps in the data represents instrument down time. Black points highlight the baseline measurements while red denote air from polluted sources.

The baselines within the Cape Point HCFC and HFC datasets were identified using the adapted AGAGE algorithm described in the Baseline Classification Algorithm in the Supplementary Information.[22,34] The algorithm relied on the iterative fitting of a second order quadratic function to the daily minima over a 121-day window.[22,34] An analysis of the 'polluted' points identified by the pollution algorithm, suggests that these were specific intrusions of anthropogenically modified air arriving at Cape Point. The pollution events at Cape Point strongly suggest the prevalence of local source of all three of these compounds. Baseline mixing ratios at Cape Point for HCFC-22, HFC-125 and HFC-152a grew by 8.36 ppt yr^{-1}, 4.10 ppt yr^{-1} and 0.71 ppt yr^{-1}, respectively, during the 2017 data acquisition window. The mean baseline mixing ratios from Cape Point were 233.50 ± 4.0 ppt, 21.95 ± 1.2 ppt, and 4.69 ± 0.5 ppt for HCFC-22, HFC-125 and HFC-152a, respectively. The baseline growth rates and mean mixing ratios reported here are in line with previous studies of the concentrations of these compounds in the atmosphere at another Southern Hemisphere site, Cape Grim (e.g. Simmonds et al.[13,22]). The baseline mixing ratios reported here were similar to reported global averages.[11,22] Any differences could be attributed to either the Southern Hemisphere location where these measurements were made, or the existence of additional, as yet unidentified, anthropogenic sources of these compounds in the region.

The measurements made at Cape Point imply that the HCFC and HFCs share a common anthropogenic source situated in the wider City of Cape Town metropole. A bivariate analysis of the HCFC and HFC measurements from Cape Point indicate a good agreement with a dominant

source to the north-east, most probably from stationary air conditioning units (Figure 4). HCFC-22 and HFC-125 appear to have greater spread of sources, based on the air sampled at Cape Point, whereas HFC-152a seems to have a single dominant source located immediately to the north of Cape Point, as shown in the bivariate plots (Figure 4c). Interestingly, the pollution marked HCFC and HFC measurements showed only marginal relationships ($r^2 < 0.5$) with known anthropogenic markers such as carbon monoxide and ^{222}Rn. The lack of relationship between HCFC and HFC mixing ratios and anthropogenic markers observed here is consistent with previous studies of this kind (e.g. Rivett et al.[42,43], Mead et al.[44], Khan et al.[45]). The HCFC-122 and HFC-125 relationship displayed weak commonality in the pollution marked air, to an r^2 of 0.37.

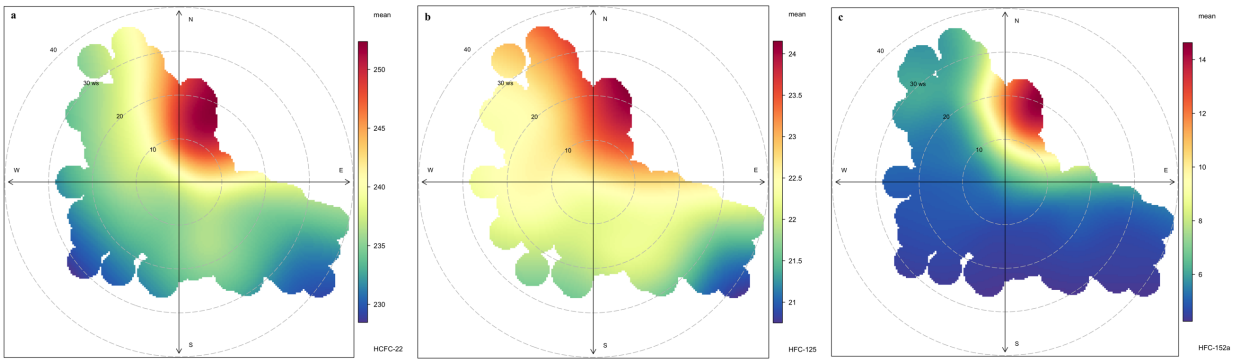

Figure 4. Bivariate plots for HCFC and HFC measurements at Cape Point. HCFC and HFC mixing ratio displayed as a function of wind speed and direction for a. HCFC-22, b. HFC-125, and c. HFC-152a.

Estimation of South African HCFC-22, HFC-125 and HFC-152a emissions using an inverse model

When used in conjunction with an inverse model, long-term atmospheric measurements from the Cape Point observatory could potentially be used to estimate South Africa's halocarbon emissions. In the absence of an annual bottom-up inventory, which South Africa is not currently required to submit, these top-down estimates could provide a useful means by which to track emissions from Africa's second largest economy. To explore this potential, we estimate South Africa's emissions of HCFC-22, HFC-125 and HFC-152a in 2017 using the hierarchical trans-dimensional Bayesian framework described in the Methods section. The estimates presented in the following discussion are based on the mean value of each posterior probability density function (PDF), with an estimation of the corresponding uncertainty taken to be the 95th percentile range (2-sigma) of the same PDF. Posterior emissions and prior scaling maps are shown in Fig. 5. A comparison of the atmospheric measurements with modelled mixing ratios is shown in Fig. S1. For each gas, the sensitivity of the inversion to changes in the magnitude of the prior is given in Fig. S2.

We estimated South African HCFC-22 emissions of 3.6 (1.3 – 8.7) Gg yr^{-1} in 2017. Our prior scaling map (Fig. 5) suggests that the measurements at Cape Point provide sufficient information for the inversion to adjust emissions from the entire country, as opposed to those exclusively within close proximity to the measurement site. Despite this, our posterior estimate is somewhat dependent on the choice of prior (Fig. S2), although for all but the smallest prior emissions field (50% of the default), the resultant uncertainty range overlaps the mean of our original estimate. As expected, the regions with large emissions typically corresponded with major urban areas, most notably the city and surroundings of Johannesburg (approximate population of 4.4 million in 2016).[46] The approximate correlation of emissions with population density is consistent with

the use of HCFC-22 as a refrigerant in stationary air-conditioning units. Simmonds et al.[13] estimated global HCFC-22 emissions of 370.3 ± 45.9 Gg yr^{-1} in 2016. When placed in context to the global burden, South Africa's HCFC-22 emissions (~1% of the global total) are relatively small. Saikawa et al.[47] estimated combined African and Middle Eastern HCFC-22 emissions of 736.4 ± 22.3 Gg yr^{-1} for 2009. Assuming that this total did not change significantly between 2009 and 2017, South Africa could account for ~10% of HCFC-22 emissions from this region. Nevertheless, emissions from the African continent as a whole are comparatively small. As a comparison, Asian Annex 5 countries emitted 213 ± 20.8 Gg yr^{-1} in the same year.[47]

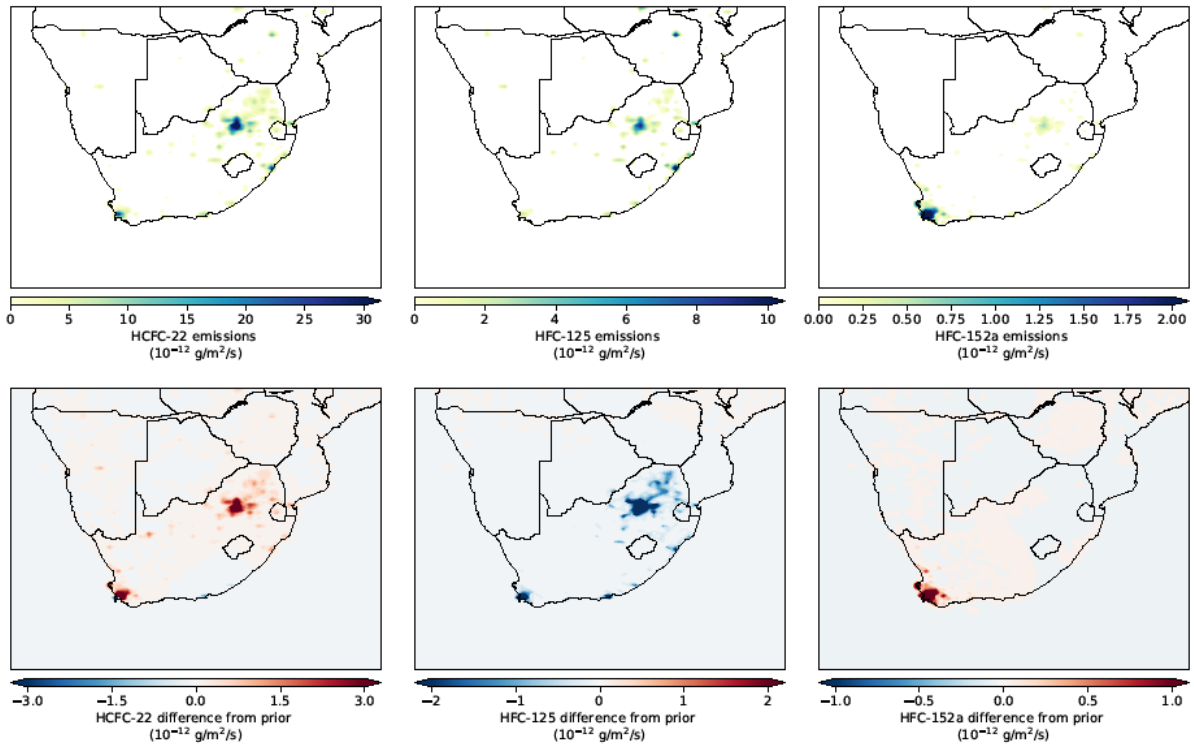

Figure 5. Top) Maps of the posterior distribution of emissions of HCFC-22, HFC-125 and HFC-152a, based on measurements from the Cape Point monitoring station. Bottom) Maps of the

difference between posterior and prior distributions of emissions, presented in the same units as above. Red indicates regions where the posterior was larger than the prior emissions field.

As consumption of HCFC-22 is reduced under the Montreal Protocol, it is widely expected that South Africa will accelerate the adoption of non-ozone depleting alternatives. R-410A (a zeotropic 50:50 blend of HFC-125 and HFC-32) is commonly cited as a replacement for HCFC-22 in refrigeration systems.[48] Our emission maps for these HCFC-22 and HFC-125 (Fig. 5) suggest a similar distribution of sources, with large emissions from Johannesburg and much smaller emissions from Cape Town. We estimate South Africa's HFC-125 emissions to be 1.6 (0.8 – 2.6) Gg yr^{-1} in 2017. Simmonds et al.[49] estimated global HFC-125 emissions of 59.7 ± 9.5 Gg yr^{-1} for 2015, hence South Africa represents approximately 2.7% of the global total. Unlike HCFC-22 and HFC-152a, our estimate for HFC-125 is insensitive to the choice of prior (Fig. S2), suggesting that the information content of the measurements is enough to provide some constraint for the whole of South Africa.

As with HFC-125, South Africa's emissions of HFC-152a might be expected to increase as it replaces ozone-depleting alternatives (e.g. HCFC-141b and HCFC-142b) in applications such as foam-blowing and as an aerosol propellant. We estimate South Africa's 2017 HFC-152a emissions to be 0.13 (0.10 – 0.19) Gg yr^{-1} which represent less than 0.4% of the global HFC-152a emissions estimated by Simmonds et al.[22] However, the model fit for this gas was poor, with a significant number of unresolved data points, possibly indicative of intermittent emissions, a strong local source or transport errors within NAME. These unresolved peaks also appear to hinder the ability of the inversion to adjust for emissions beyond Cape Town, though the posterior distribution is consistent with the HFC-152a bivariate plot in Fig. 4c, which suggests a single strong source to the north of Cape Point. The results of the sensitivity study

show the inversion to be highly dependent on the choice of prior, consistent with the poor sensitivity of the inversion to distant sources. The uncertainty bounds for both small (50% of the default) and large (200% of the default) priors do not overlap with the mean original estimate.

The sensitivity of our HCFC-22 and HFC-152a emissions estimates to changes in the magnitude of the prior suggests that the inversion is insensitive to sources from the East of South Africa (e.g. those many hundreds of kilometres from Cape Point). To assess how robust our estimates are for sources near to the observatory (including Cape Town but excluding Johannesburg), a second set of emissions were estimated using the sub-domain shown in Fig. S3. The South West South Africa (SWSA) domain extends to a maximum latitude and longitude of 30 °S and 24 °E, respectively. A summary of the results is shown in Fig. S4. Emissions of HCFC-22 and HFC-125 were very insensitive to the choice of prior. In contrast, HFC-152a remained sensitive to increases in the magnitude of the prior, suggesting that the presence of a persistent unresolvable signal results in a less robust estimate for this gas. We estimate SWSA emissions of 0.37 (0.20 – 0.55) Gg yr^{-1}, 0.10 (0.06 – 0.15) Gg yr^{-1} and 0.08 (0.07 – 0.09) Gg yr^{-1}, accounting for 10%, 6% and 61% of South Africa's total emissions, for HCFC-22, HFC-125 and HFC-152a respectively.

As an Article-5 country, South Africa is not required to publish a detailed inventory of its greenhouse gas emissions.[14] Except for consumption statistics submitted as part of its Montreal Protocol commitments, South Africa's HCFC and HFC emissions are poorly defined. As per the HPMP, South Africa was required to freeze its HCFC consumption by 2013 (relative to a 2009/10 baseline) followed by successive cuts leading to a complete phase-out by 2040. South Africa is also in the process of ratifying the Kigali Amendment to the Montreal Protocol, which sets out plans to reduce global emissions of HFCs and came into effect on January 1st 2019.

However, South Africa will not be required to make its first reductions in the production or consumption of HFCs until 2040. Given the current and impending regulations imposed on South Africa's halocarbon emissions, in the absence of a nationwide monitoring programme for these compounds, plausible estimates of the country's emissions are useful. Ongoing atmospheric measurements of key HCFC and HFC mixing ratios at Cape Point provide a valuable means by which to verify South Africa's progress under the Kigali Amendment.

Further work is required to verify the results of this study, if these estimates are to form a reliable means of validation for future inventory work. Particular attention to better understand the local sources of HFC-152a is required, as it is possible that a strong source within close proximity of Cape Point could mask emissions from further afield. The usefulness of Cape Point as a means by which to estimate South Africa's halocarbon emissions is also likely to increase as the dataset grows. In particular, more data collected during the Southern Hemisphere autumn and winter months - which corresponds with a maximum in the sensitivity of the site to terrestrial sources – would be highly beneficial. In addition, further measurements from the East of the country and Johannesburg in particular would improve the ability of the inversion to accurately constrain sources from the entirety of South Africa.

ASSOCIATED CONTENT

Code availability

The inverse model code used in this study is available upon request from Matt Rigby (Matt.Rigby@bristol.ac.uk). The NAME model is available upon request to the UK Met Office.

AUTHOR INFORMATION

Corresponding author

*email: D.E.S. d.e.shallcross@bristol.ac.uk, Tel: +44 117 928 7796

Notes

The authors declare no competing financial interest.

ACKNOWLEDGEMENTS

We thank a variety of funders under whose auspices this work was carried out including Bristol ChemLabS Outreach, Primary Science Teaching Trust (MAHK) and NERC grants NE/M014851/1 and NE/I027282/1 (Daniel Say). The authors would like to thank the Universities of Bristol and the Western Cape for their support. The authors would like to thank William J Whittaker for his assistance in decoding the AGAGE pollution algorithm.

REFERENCES

(1) Derwent, R. G.; Volz-Thomas, A. The Tropospheric Lifetimes of Halocarbons and Their Reactions with OH Radicals: An Assessment Based on the Concentration of ^{14}CO. In

428 *UNEP/WMO Scientific Assessment of Stratospheric Ozone*; 1989; p Appendix.

429(2) Liu, R.; Huie, R. E.; Kurylo, M. J. Rate Constants for the Reactions of the OH Radical
430 with Some Hydrochlorofluorocarbons over the Temperature Range 270-400 K.
431 *J.Phys.Chem.* **1990**, *94* (7), 3247–3249. https://doi.org/10.1021/j100371a004.

432(3) Fisher, D. A.; Hales, C. H.; Filkin, D. L.; Ko, M. K. W.; Sze, N. D.; Connell, P. S.;
433 Wuebbles, D. J.; Isaksen, I. S. A.; Stordal, F. Model Calculations of the Relative Effects of
434 CFCs and Their Replacements on Stratospheric Ozone. *Nature* **1990**, *344* (6266), 508–
435 512. https://doi.org/10.1038/344508a0.

436(4) Naik, V.; Jain, A. K.; Patten, K. O.; Wuebbles, D. J. Consistent Sets of Atmospheric
437 Lifetimes and Radiative Forcings on Climate for CFC Replacements: HCFCs and HFCs.
438 *J. Geophys. Res. Atmos.* **2000**, *105* (D5), 6903–6914.
439 https://doi.org/10.1029/1999JD901128.

440(5) Velders, G. J. M. M.; Fahey, D. W.; Daniel, J. S.; McFarland, M.; Andersen, S. O. The
441 Large Contribution of Projected HFC Emissions to Future Climate Forcing. *Proc. Natl.*
442 *Acad. Sci. U. S. A.* **2009**, *106* (27), 10949–10954.
443 https://doi.org/10.1073/pnas.0902817106.

444(6) Papanastasiou, D. K.; Beltrone, A.; Marshall, P.; Burkholder, J. B. Global Warming
445 Potential Estimates for the C_1 – C_3 Hydrochlorofluorocarbons (HCFCs) Included in the
446 Kigali Amendment to the Montreal Protocol. *Atmos. Chem. Phys.* **2018**, *18*, 6317–6330.

447(7) UNEP - Ozone Secretariat. *Amendement to the Montreal Protocol on Substances That*
448 *Deplete the Ozone Layer: Report*; Copenhagen, 1992.

449(8) UNEP - Ozone Secretariat. *Amendment to the Montreal Protocol on Substances That*
450 *Deplete the Ozone Layer: Report*; Kigali, 2016.

451(9) WMO. *Scientific Assessment of Ozone Depletion: 2014*; World Meteorological
452 Organization, 2014.

453(10) Rinsland, C. P.; Chiou, L.; Boone, C.; Bernath, P.; Mahieu, E. First Measurements of the
454 HCFC-142b Trend from Atmospheric Chemistry Experiment (ACE) Solar Occultation
455 Spectra. *J. Quant. Spectrosc. Radiat. Transf.* **2009**, *110* (18), 2127–2134.
456 https://doi.org/10.1016/j.jqsrt.2009.05.011.

457(11) Simmonds, P. G.; Rigby, M.; McCulloch, A.; O'Doherty, S. J.; Young, D.; Mühle, J.;
458 Krummel, P. B.; Steele, L. P.; Fraser, P. J.; Manning, A. J.; et al. Changing Trends and
459 Emissions of Hydrochlorofluorocarbons (HCFCs) and Their Hydrofluorocarbon (HFCs)
460 Replacements. *Atmos. Chem. Phys.* **2017**, *17* (7), 4641–4655. https://doi.org/10.5194/acp-
461 17-4641-2017.

462(12) Burkholder, J. B.; Cox, R. A.; Ravishankara, A. R. Atmospheric Degradation of Ozone
463 Depleting Substances, Their Substitutes, and Related Species. *Chem. Rev.* **2015**, *115* (10),
464 3704–3759. https://doi.org/10.1021/cr5006759.

465(13) Simmonds, P. G.; Rigby, M.; McCulloch, A.; Vollmer, M. K.; Henne, S.; Mühle, J.;
466 O'Doherty, S. J.; Manning, A. J.; Krummel, P. B.; Fraser, P. J.; et al. Recent Increases in
467 the Atmospheric Growth Rate and Emissions of HFC-23 (CHF_3) and the Link to HCFC-22
468 ($CHClF_2$) Production. *Atmos. Chem. Phys.* **2018**, *18* (6), 4153–4169.
469 https://doi.org/10.5194/acp-18-4153-2018.

(14) Graziosi, F.; Arduini, J.; Furlani, F.; Giostra, U.; Kuijpers, L. J. M.; Montzka, S. A.; Miller, B. R.; O'Doherty, S. J.; Stohl, A.; Bonasoni, P.; et al. European Emissions of HCFC-22 Based on Eleven Years of High Frequency Atmospheric Measurements and a Bayesian Inversion Method. *Atmos. Environ.* **2015**, *112*, 196–207. https://doi.org/10.1016/j.atmosenv.2015.04.042.

(15) Aucott, M. L.; McCulloch, A.; Graedel, T. E.; Kleiman, G.; Midgley, P.; Li, Y.-F. Anthropogenic Emissions of Trichloromethane (Chloroform CHCl_{3\}) and Chlorodifluoromethane (HCFC-22): Reactive Chlorine Emissions Inventory. *J. Geophys. Res.* **1999**, *104* (D7), 8405–8415. https://doi.org/10.1029/1999JD900053.

(16) Xiang, B.; Patra, P. K.; Montzka, S. A.; Miller, S. M.; Elkins, J. W.; Moore, F. L.; Atlas, E. L.; Miller, B. R.; Weiss, R. F.; Prinn, R. G.; et al. Global Emissions of Refrigerants HCFC-22 and HFC-134a: Unforeseen Seasonal Contributions. *Proc. Natl. Acad. Sci.* **2014**, *111* (49), 17379–17384. https://doi.org/10.1073/pnas.1417372111.

(17) Forster, P.; Ramaswamy, V.; Artaxo, P.; Berntsen, T.; Betts, R.; Fahey, D. W.; Haywood, J.; Lean, J.; Lowe, D. C.; Myhre, G.; et al. Climate Change 2007: The Physical Science Basis. Contribution of Working Group I to the Fourth Assessment Report of the Intergovernmental Panel on Climate Change. Chapter 2: Changes in Atmospheric and Radiative Forcing. *Cambridge Univ. Press* **2007**, 129–234. https://doi.org/10.1103/PhysRevB.77.220407.

(18) O'Doherty, S. J.; Miller, B. R.; Mühle, J.; McCulloch, A.; Simmonds, R. G.; Manning, A. J.; Reimann, S.; Vollmer, M. K.; Greally, B. R.; Prinn, R. G.; et al. Global and Regional Emissions of HFC-125 (CHF2CF3) from in Situ and Air Archive Atmospheric

492 Observations at AGAGE and SOGE Observatories. *J. Geophys. Res. Atmos.* **2009**, *114*
493 (23). https://doi.org/10.1029/2009JD012184.

494(19) McCulloch, A. Evidence for Improvements in Containment of Fluorinated Hydrocarbons
495 during Use: An Analysis of Reported European Emissions. *Environ. Sci. Policy* **2009**, *12*
496 (2), 149–156. https://doi.org/10.1016/j.envsci.2008.12.003.

497(20) Lunt, M. F.; Rigby, M.; Ganesan, A. L.; Manning, A. J.; Prinn, R. G.; O'Doherty, S.;
498 Mühle, J.; Harth, C. M.; Salameh, P. K.; Arnold, T.; et al. Reconciling Reported and
499 Unreported HFC Emissions with Atmospheric Observations. *Proc. Natl. Acad. Sci.* **2015**,
500 *112* (19), 5927–5931. https://doi.org/10.1073/pnas.1420247112.

501(21) Li, P.; Mühle, J.; Montzka, S. A.; Oram, D. E.; Miller, B. R.; Tanhua, T. Global Annual
502 Mean Atmospheric Histories , Growth Rates and Seawater Solubility Estimations of the
503 Halogenated Compounds PFC-14 and PFC-116. *Ocean Sci. Discuss.* **2018**, No. August, 1–
504 51.

505(22) Simmonds, P. G.; Rigby, M.; Manning, A. J.; Lunt, M. F.; O'Doherty, S. J.; McCulloch,
506 A.; Fraser, P. J.; Henne, S.; Vollmer, M. K.; Mühle, J.; et al. Global and Regional
507 Emissions Estimates of 1,1-Difluoroethane (HFC-152a, CH3CHF2) from in Situ and Air
508 Archive Observations. *Atmos. Chem. Phys.* **2016**, *16* (1), 365–382.
509 https://doi.org/10.5194/acp-16-365-2016.

510(23) NEDLAC. *Hydrochlorofluorocarbons (HCFC) Phase Out Plan for South Africa*; National
511 Economic Development and Labour Council, Departmenet of Environmental Affairs:
512 Johannesburg, 2012.

513(24) Labuschagne, C.; Kuyper, B.; Brunke, E.; Spuy, D. Van Der; Martin, L.; Mbambalala, E.;
514 Khan, M. A. H.; Davies-coleman, M. T.; Shallcross, D. E.; Joubert, W. A Review of Four
515 Decades of Atmospheric Trace Gas Measurements at Cape Point, South Africa. *Trans. R.*
516 *Soc. South Africa* **2018**, 1–20. https://doi.org/10.1080/0035919X.2018.1477854.

517(25) Tyson, P. D.; Preston-Whyte, R. A. *The Weather and Climate of Southern Africa*; Oxford
518 University Press Southern Africa: Cape Town, 2000.

519(26) Preston-Whyte, R. A.; Tyson, P. D. *The Atmosphere and Weather of Southern Africa*;
520 Oxford University Press: Oxford, 1993.

521(27) Garstang, M.; Tyson, P. D.; Edwards, M.; Kallberg, P.; Lindesay, J. A. Horizontal and
522 Vertical Transport of Air over Southern Africa. *J. Geophys. Res.* **1996**, *101* (D19), 23721–
523 23736. https://doi.org/10.1029/95JD00844.

524(28) Brunke, E.; Walters, C.; Mkololo, T.; Martin, L. G.; Labuschagne, C.; Silwana, B.; Slemr,
525 F.; Weigelt, A.; Ebinghaus, R.; Somerset, V. Mercury in the Atmosphere and in Rainwater
526 at Cape Point, South Africa. *Atmos. Environ.* **2016**, *125*, 24–32.
527 https://doi.org/10.1016/j.atmosenv.2015.10.059.

528(29) Simmonds, P. G.; O'Doherty, S. J.; Nickless, G.; Sturrock, G. A.; Swaby, R.; Knight, P.;
529 Ricketts, J.; Woffendin, G.; Smith, R. Automated Gas Chromatograph/Mass Spectrometer
530 for Routine Atmospheric Field Measurements of the CFC Replacement Compounds, the
531 Hydrofluorocarbons and Hydrochlorofluorocarbons. *Anal. Chem.* **1995**, *67* (4), 717–723.
532 https://doi.org/10.1021/ac00100a005.

533(30) O'Doherty, S. J.; Simmonds, P. G.; Nickless, G.; Betz, W. R. Evaluation of Carboxen

534 Carbon Molecular Sieves for Trapping Replacement Chlorofluorocarbons. *J. Chromatogr.*
535 **1993**, *630*, 265–274. https://doi.org/10.2989/02577619209504717.

536(31) Sturrock, G. A.; Porter, L. W.; Fraser, P. J. In Situ Measurement of CFC Replacement
537 Chemicals and Other Halocarbons at Cape Grim: The AGAGE GC-MS Program. In
538 *Baseline 97–98*; Tindale, N. W., Derek, N., Francey, R. J., Eds.; Bureau of Meteorology,
539 CSIRO: Melbourne, Victoria, 2001; pp 43–49.

540(32) Miller, B. R.; Weiss, R. F.; Salameh, P. K.; Tanhua, T.; Greally, B. R.; Mühle, J.;
541 Simmonds, P. G. Medusa: A Sample Preconcentration and GC-MS Detector System for in
542 Situ Measurements of Atmospheric Trace Halocarbons, Hydrocarbons and Sulfur
543 Compounds. *Anal. Chem.* **2008**, *80* (1), 1536–1545. https://doi.org/10.1021/ac702084k.

544(33) Arnold, T.; Mühle, J.; Salameh, P. K.; Harth, C. M.; Ivy, D. J.; Weiss, R. F. Automated
545 Measurement of Nitrogen Trifluoride in Ambient Air. *Anal. Chem.* **2012**, *84*, 4798–4804.
546 https://doi.org/10.1021/ac300373e.

547(34) O'Doherty, S. J.; Simmonds, P. G.; Cunnold, D. M.; Wang, H. J.; Sturrock, G. A.; Fraser,
548 P. J.; Ryall, D. B.; Derwent, R. G.; Weiss, R. F.; Salameh, P. K.; et al. In Situ Chloroform
549 Measurements at Advanced Global Atmospheric Gases Experiment Atmospheric Research
550 Stations from 1994 to 1998. *J. Geophys. Res. Atmos.* **2001**, *106* (D17), 20429–20444.
551 https://doi.org/10.1029/2000JD900792.

552(35) Manning, A. J.; O'Doherty, S. J.; Jones, A. R.; Simmonds, P. G.; Derwent, R. G.
553 Estimating UK Methane and Nitrous Oxide Emissions from 1990 to 2007 Using an
554 Inversion Modeling Approach. *J. Geophys. Res. Atmos.* **2011**, *116* (2), 1–19.
555 https://doi.org/10.1029/2010JD014763.

556(36) Lunt, M. F.; Rigby, M.; Ganesan, A. L.; Manning, A. J. Estimation of Trace Gas Fluxes
557 with Objectively Determined Basis Functions Using Reversible-Jump Markov Chain
558 Monte Carlo. *Geosci. Model Dev.* **2016**, *9* (9), 3213–3229. https://doi.org/10.5194/gmd-9-
559 3213-2016.

560(37) Ganesan, A. L.; Rigby, M.; Zammit-Mangion, A.; Manning, A. J.; Prinn, R. G.; Fraser, P.
561 J.; Harth, C. M.; Kim, K. R.; Krummel, P. B.; Li, S.; et al. Characterization of
562 Uncertainties in Atmospheric Trace Gas Inversions Using Hierarchical Bayesian Methods.
563 *Atmos. Chem. Phys.* **2014**, *14* (8), 3855–3864. https://doi.org/10.5194/acp-14-3855-2014.

564(38) Lunt, M. F.; Park, S.; Li, S.; Henne, S.; Manning, A. J.; Ganesan, A. L.; Simpson, I. J.;
565 Blake, D. R.; Liang, Q.; O'Doherty, S.; et al. Continued Emissions of the Ozone-
566 Depleting Substance Carbon Tetrachloride From Eastern Asia. *Geophys. Res. Lett.* **2018**,
567 *4*, 423–430. https://doi.org/10.1029/2018GL079500.

568(39) Say, D.; Ganesan, A. L.; O'Doherty, S.; Rigby, M.; Lunt, M. F.; Harth, C.; Manning, A. J.;
569 Krummel, P. B.; Bauguitte, S. J.-B. Atmospheric Observations and Emission Estimates of
570 Ozone-Depleting Chlorocarbons from India. *Atmos. Chem. Phys. Discuss.* **2018**.

571(40) Raupach, M. R.; Rayner, P. J.; Paget, M. Regional Variations in Spatial Structure of
572 Nightlights, Population Density and Fossil-Fuel CO2emissions. *Energy Policy* **2010**, *38*
573 (9), 4756–4764. https://doi.org/10.1016/j.enpol.2009.08.021.

574(41) Rigby, M.; Prinn, R. G.; O'Doherty, S. J.; Miller, B. R.; Ivy, D.; Mühle, J.; Harth, C. M.;
575 Salameh, P. K.; Arnold, T.; Weiss, R. F.; et al. Recent and Future Trends in Synthetic
576 Greenhouse Gas Radiative Forcing. *Geophys. Res. Lett.* **2014**, *41* (7), 2623–2630.
577 https://doi.org/10.1002/2013GL059099.

578(42) Rivett, A. C.; Martin, D.; Nickless, G.; Simmonds, P. G.; O'Doherty, S. J.; Gray, D. J.;
579 Shallcross, D. E. In Situ Gas Chromatographic Measurements of Halocarbons in an Urban
580 Environment. *Atmos. Environ.* **2003**, *37* (16), 2221–2235. https://doi.org/10.1016/S1352-
581 2310(03)00148-1.

582(43) Rivett, A. C.; Martin, D.; Gray, D. J.; Price, C. S.; Nickless, G.; Simmonds, P. G.;
583 O'Doherty, S. J.; Greally, B. R.; Knights, A.; Shallcross, D. E. The Role of Volatile
584 Organic Compounds in the Polluted Urban Atmosphere of Bristol, England. *Atmos. Chem.*
585 *Phys.* **2003**, *3* (4), 1165–1176. https://doi.org/10.5194/acp-3-1165-2003.

586(44) Mead, M. I.; Khan, M. A. H.; Bull, I. D.; White, I. R.; Nickless, G.; Shallcross, D. E.
587 Stable Carbon Isotope Analysis of Selected Halocarbons at Parts per Trillion
588 Concentration in an Urban Location. *Environ. Chem.* **2008**, *5* (5), 340–346.
589 https://doi.org/10.1071/EN08037.

590(45) Khan, M. A. H.; Mead, M. I.; White, I. R.; Golledge, B.; Nickless, G.; Knights, A.;
591 Martin, D.; Rivett, A. C.; Greally, B. R.; Shallcross, D. E. Year-Long Measurements of C_1-
592 C_3 Halocarbons at an Urban Site and Their Relationship with Meteorological Parameters.
593 *Atmos. Sci. Lett.* **2009**, *10*, 75–86. https://doi.org/10.1002/asl.

594(46) CIESEN. Gridded Population Of the World (gpw), V4.

595(47) Saikawa, E.; Rigby, M.; Prinn, R. G.; Montzka, S. A.; Miller, B. R.; Kuijpers, L. J. M.;
596 Fraser, P. J. B.; Vollmer, M. K.; Saito, T.; Yokouchi, Y.; et al. Global and Regional
597 Emission Estimates for HCFC-22. *Atmos. Chem. Phys.* **2012**, *12* (21), 10033–10050.
598 https://doi.org/10.5194/acp-12-10033-2012.

(48) Spatz, M. W.; Motta, S. F. Y. An Evalution of Options for Replacing HCFC-22 in Medium Temperature Refrigeration Systems. *Int. J. Refrig.* **2004**, *27* (5), 475–483. https://doi.org/10.1016/j.ijrefrig.2004.02.009.

(49) Simmonds, P. G.; Rigby, M.; McCulloch, A.; O'Doherty, S.; Young, D.; Mühle, J.; Krummel, P. B.; Steele, P.; Fraser, P. J.; Manning, A. J.; et al. Changing Trends and Emissions of Hydrochlorofluorocarbons (HCFCs) and Their Hydrofluorocarbon (HFCs) Replacements. *Atmos. Chem. Phys.* **2017**, *17* (7), 4641–4655. https://doi.org/10.5194/acp-17-4641-2017.

SUPPLEMENTARY INFORMATION

S1 Baseline classification algorithm

The baseline classification algorithm uses a three-step process to determine a baseline fit. A 121-day rolling window, consisting of measurements for 60 days either side of each sampling day was used in the baseline fit. In the first step the daily minima over the whole 121-day

618window were determined. A second order polynomial was then fitted to the daily minima. The
619polynomial fit was subtracted from each measurement in the 121-day window, creating a matrix
620of distances from the polynomial fit. The median of the distances was calculated, which has been
621shown to be less sensitive to outliers compared to the mean.[34] Only distance values below the
622median were used in the variability calculation. The variability of the distance matrix was
623determined by the root mean square (RMS) deviation (σ) of the distances. Values in the distance
624dataset larger than 3σ (tunable) above the median were marked as 'polluted'. Consequently, all
625the other values were marked as baseline. Only the marked data ('pollution' and 'baseline') for
626the day of the event were retained and the window moved to the next sampling day.

627 The baseline fit was improved in the second step, which was identical to the first step,
628described above, except that the data marked as 'polluted' were excluded. The repeat of the
629procedure without the 'polluted' marked data is important especially for highly polluted air, as
630extremely elevated observations can bias the median. Measurements that were between 2σ and
6313σ in this second round were marked as 'possibly polluted'.

632 The third step analysed the data marked as 'possibly polluted'. A test was performed to
633examine if a point marked as 'possibly polluted' was adjacent to 'polluted' data point. If there
634was adjacency, then the 'possibly polluted' data point was reclassified as 'polluted'. If
635measurements were not marked as polluted these were then considered as baseline.

636

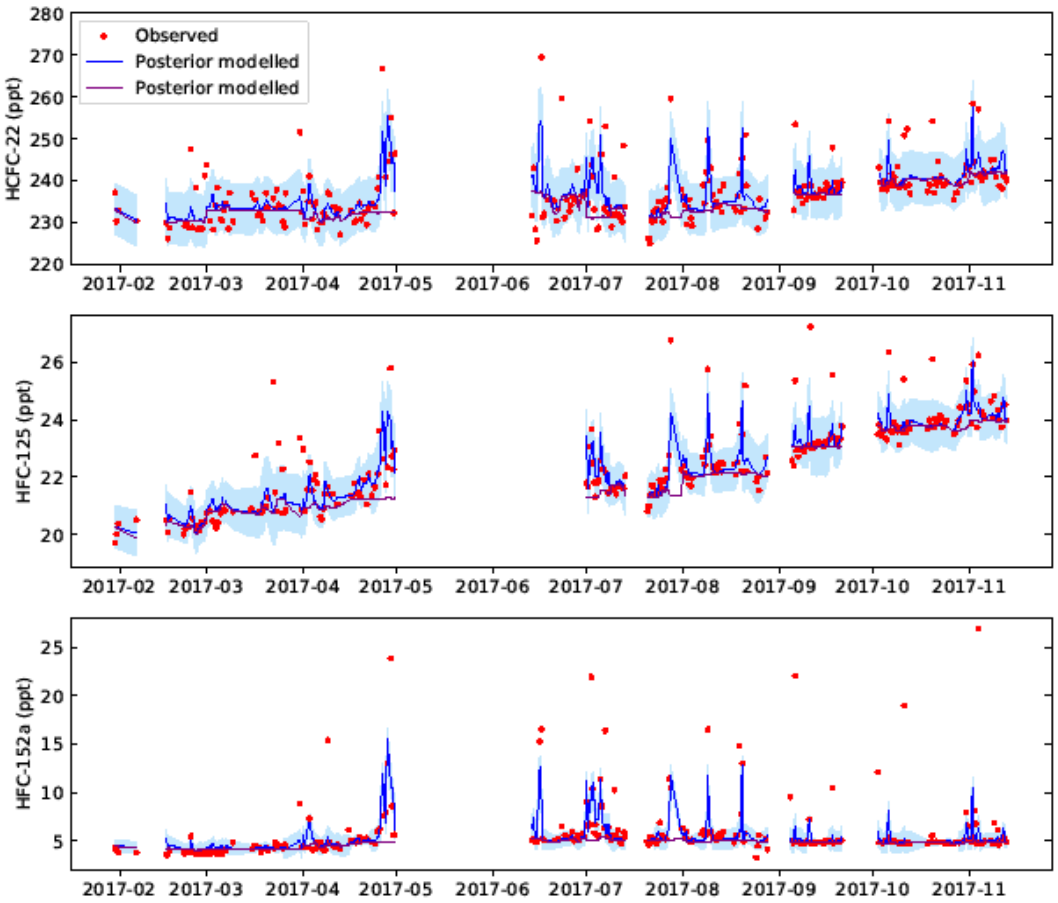

637

638 **Figure S1**: A comparison of measured (red points, ppt) and modelled (blue line, ppt) mole
639 fractions at Cape Point. Observations and NAME back-trajectories were binned into 12-hour
640 averages. Model uncertainty (95th percentile confidence interval) is represented by the pale blue
641 shading. The modelled baseline (purple line) is also shown.
642

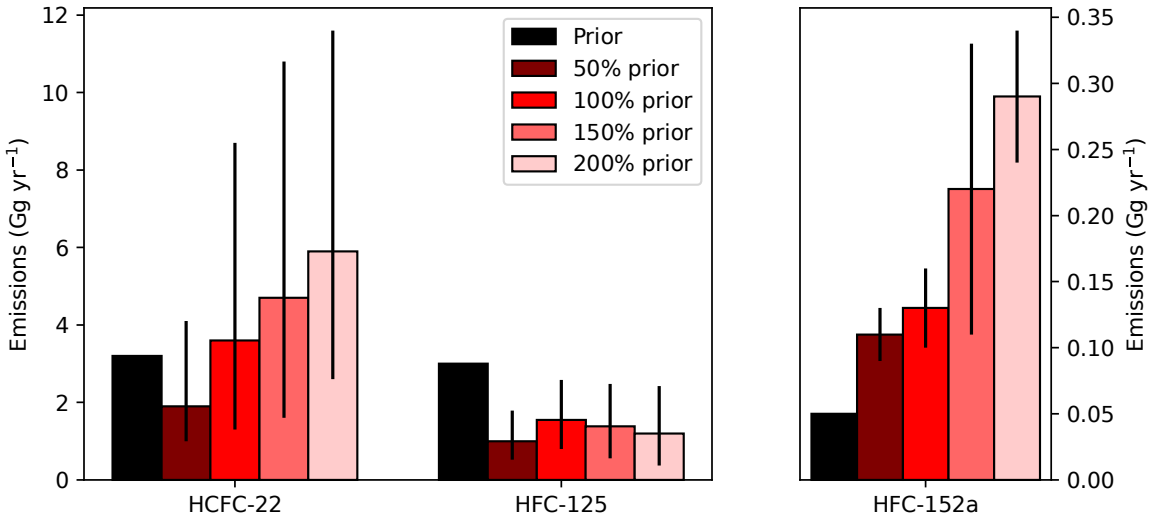

643

644 **Figure S2:** Sensitivity plots showing the change in posterior emissions as a result of scaling
645 (50% - 200%) of the prior. Error bars represent the 95th percentile confidence interval of the
646 posterior PDFs.

647

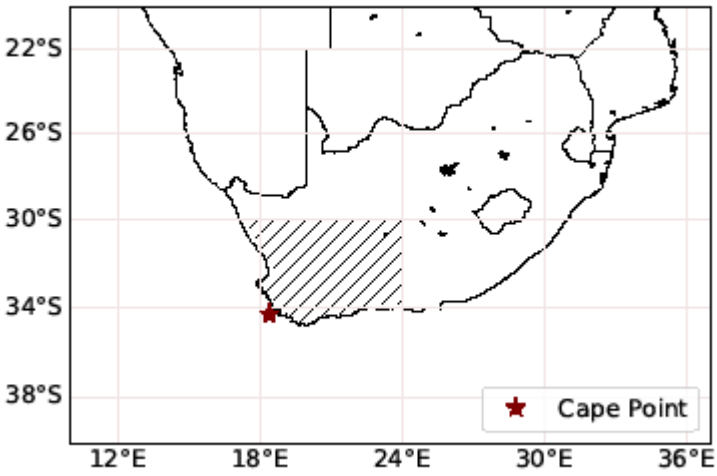

648

649 **Figure S3:** Plot showing the reduced domain for South West South Africa (SWSA, hatched
650 lines). The Cape Point observatory is also shown (red star).

651

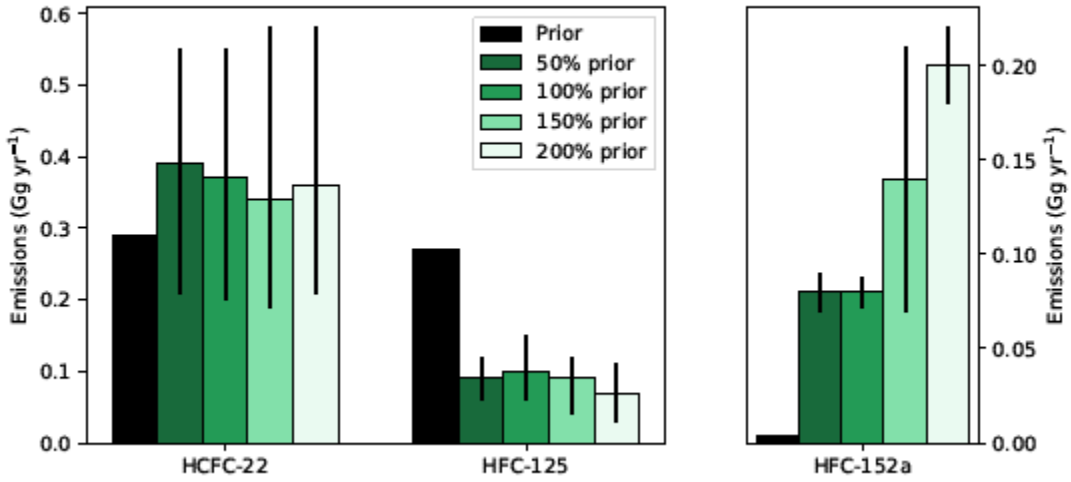

Figure S4: Sensitivity plots showing the change in posterior emissions for the reduced South West South Africa domain as a result of scaling (50% - 200%) of the prior. Error bars represent the 95th percentile confidence interval of the posterior PDFs.